Peer reviewed version

License (if available):
CC BY-NC-ND

Link to published version (if available):
[10.1016/j.sbi.2020.06.001](10.1016/j.sbi.2020.06.001)

Link to publication record in Explore Bristol Research
PDF-document

University of Bristol - Explore Bristol Research
General rights

Enzyme Evolution and the Temperature Dependence of Enzyme Catalysis

Vickery L. Arcus[1*], Marc W. van der Kamp[2], Christopher R. Pudney[3] & Adrian J. Mulholland[4*]

[1]School of Science, University of Waikato, Hamilton 3240, New Zealand.

[2]School of Biochemistry, University of Bristol, Biomedical Sciences building, University Walk, Bristol BS8 1TD, UK.

[3]Department of Biology and Biochemistry, University of Bath, Bath BA2 7BA, UK.

[4]Centre for Computational Chemistry, School of Chemistry, Cantock's Close, University of Bristol, BS8 1TS, UK.

Corresponding authors

vic.arcus@waikato.ac.nz

adrian.mulholland@bristol.ac.uk

Abstract (100-120 words)

Experiments and biomolecular simulations are revealing new and unexpected details of how enzymes are adapted to specific temperatures. These findings are elucidating enzyme evolutionary trajectories and offer great promise for design and engineering of natural and artificial enzymes. They also have implications for understanding responses of larger scale biological temperature dependence, relevant for understanding the effects of climate change on ecosystems. We review recent work on the temperature dependence of enzyme-catalysed reaction rates and the implications for enzyme evolution. Evidence from kinetic isotope effects, temperature dependent reaction rates, molecular dynamics simulations and thermodynamics provides new insights into enzyme thermoadaptation and evolution.

Introduction

Enzymes compress the vast timescale over which chemical reactions take place ($10^{-9} - 10^{17}$ s) onto timescales needed for life ($10^{-3} - 10^5$ s). This involves enzyme-catalysed rate enhancements of up to 10^{20} [1]. Experiments and molecular simulations have revealed mechanisms for enzyme-catalysed reactions and details of the fundamental origins of catalysis. Life not only faces the challenge of how to increase chemical reaction rates, but also of ensuring that the rates are appropriate for the physical conditions in which organisms live. Life occupies almost every available niche on the planet and thus, enzymes have evolved to operate at diverse temperatures (between –20°C and +120°C); enzymes have been tailored by evolution to operate optimally at the temperature(s) encountered by the organisms in which they function. For example, enzymes adapted to hot environments show significantly different optimum temperatures than those from organisms adapted to the cold; it is increasingly clear that these activity differences are not due only to differences in stability, but rather reflect a tailoring of enzyme dynamics by evolution.

Research into the temperature dependence of enzyme catalysed reaction rates has a rich history that goes back at least 100 years [2]. A recent confluence of experiment and computation [3-5••,6,7••] points towards an emerging consensus regarding the molecular mechanisms for enzyme catalysis and the evolutionary adaptations that have occurred with changing environmental temperatures. Temperature also affects molecular dynamics and the relationship between dynamics and catalysis is controversial [8,9]. Advances in computational simulations along with new experimental approaches are being combined to address the relationship between enzyme catalysis, dynamics, temperature and evolution [10••-12].

Temperature and Enzyme-catalysed reaction rates

Enzyme-catalysed reaction rates are described well by transition state theory [13,14] (equation 1, the Eyring equation). The Eyring equation expresses the rate constant in terms of the free energy difference between the reactants (ground state) and the transition state ($\Delta G^{\ddagger} = \Delta H^{\ddagger} - T\Delta S^{\ddagger}$) modified by the transmission coefficient $\gamma(T)$ and the barrier-less frequency $k_B T/h$ where k_B and h are the Boltzmann and Planck constants respectively. This predicts an exponential relationship between the chemical rate constant, k_{cat}, and temperature. Wolfenden has suggested that if life evolved at elevated temperatures where uncatalysed reaction rates and their catalysed counterparts are relatively close [12] (Figure 1A), then as temperatures cooled,

enzymes must have evolved to reduce $\Delta H^{\ddagger}$ to escape the exponential decline in rates with a decrease in temperature. This has been described as escaping the "tyranny of Arrhenius" as temperatures change over evolutionary time or organisms migrate between different environments [15].

$$k_{cat} = \gamma(T) \frac{k_B T}{h} e^{\left(\frac{-\Delta G^{\ddagger}(T)}{k_B T}\right)} = \gamma(T) \frac{k_B T}{h} e^{\left(\frac{\Delta S^{\ddagger}}{k_B}\right)} e^{\left(\frac{-\Delta H^{\ddagger}}{k_B T}\right)} \qquad (1)$$

Several investigators have observed that enzymes achieve the required reduction in $\Delta H^{\ddagger}$ for the reaction at the expense of $\Delta S^{\ddagger}$ (an enthalpy-entropy trade off). Thermophilic enzymes are often much less active at lower temperatures than their mesophilic homologues (Figure 1A) and this has been attributed to a tradeoff between enthalpy and entropy [16]. Similarly, psychrophilic enzymes show significant activity at low temperatures at which their mesophilic and thermophilic counterparts often show very low activity. Particularly for psychrophilic enzymes (enzymes from organisms whose environmental temperatures are below ~15 °C), the tradeoff was previously thought to come at the expense of enzyme stability whereby psychrophilic enzymes were regarded as generally very flexible and much less stable than their thermologues. Results from directed evolution and design, show that this view is overly simplistic. For example, a psychrophilic enzyme has been made more stable without loss of psychrophilic activity [17], and a thermophilic enzyme has been engineered to be more active at mesophilic temperatures without loss of stability [6]. Indeed, the role of neutral drift may be an important factor in the reduction of stability for psychrophilic enzymes in the absence of selection for stability at higher temperatures [18]. Many psychrophilic enzymes are properly folded and active catalysts at temperatures above their optima. Recent results for psychrophilic enzymes are providing insights into the molecular details of enzyme evolution [19,20].

Psychrophilic Enzymes

It has long been thought that thermophilic enzymes are generally more rigid, and psychrophilic enzymes are generally less rigid, than their mesophilic counterparts when compared at the same temperature. This belief gave rise to the 'corresponding states' hypothesis, [21] i.e. that each enzyme has similar flexibility and dynamics at their respective environmental temperatures (Figure 1A). The molecular origins of the enthalpy-entropy tradeoff (e.g. to achieve high activity at low temperatures) have been suggested to reside in the active site, with psychrophiles having more flexible active sites compared to their thermologues [22]. However,

recent experimental and computational results from Brandsdal, Åqvist and colleagues show that the increased flexibility of psychrophiles resides at the periphery of the enzyme [23]. In an elegant set of computational experiments using molecular dynamics simulations with empirical valence bond (EVB) models, they showed that increasing rigidity at the periphery of an enzyme converts it from a psychrophile to a mesophile [11]. They have gone further to use this approach to engineer psychrophilic and mesophilic elastase enzymes [5••,24•].

An intriguing feature of psychrophilic enzymes is that their temperature optima (T_{opt}) often lie far below their unfolding temperatures (T_M) [25]. This is the result of non-linear Arrhenius behaviour which is not due to denaturation. The trivial explanation for this behaviour is a change in the rate determining step with temperature, however this can often be excluded. This is a conundrum and has led to hypotheses about the possible molecular origins of non-linear Arrhenius behaviour [26-28].

Non-linear Arrhenius Behaviour

There is increasing evidence that the temperature dependence of many enzyme-catalysed reactions does not follow simple (linear) Arrhenius behaviour, but rather shows significant curvature, passing through a temperature of optimal activity (T_{opt}). Such behaviour is accounted for by Macromolecular Rate Theory (MMRT, see below) [29]. Evidence for such behaviour has been accumulating and has been noted by many investigators. Models presented to account for this behaviour show some notable common features. For example, Daniel and Danson put forward a model for the temperature dependence of enzyme-catalysed rates that included both the catalytic and unfolding rate constants [30]. Their model (based on numerous experimental datasets for different enzymes) showed non-linear Arrhenius behaviour for many enzymes "at zero time" – i.e. in the absence of denaturation. Central to their model is that they postulate two conformations in equilibrium for the native enzyme, one active and the other inactive. This is reminiscent of the Monod-Wyman-Changeux (MWC) and Koshland-Nemethy-Filmer (KNF) models for allosteric regulation of enzymes with two states [31]. Truhlar and Kohen showed that a more reactive and less reactive state in equilibrium account for non-linear Arrhenius behaviour [28]. If enzymes sample at least two conformational states in the ground state for the reaction and that this is compressed into a single conformation at the transition state, then this is sufficient to explain curvature in Arrhenius plots (Figure 1B). Glowacki and colleagues also invoke two conformations with different reactivities to account for anomalous

temperature dependence of some kinetic isotope effects [9]. Two different conformations in the ground state with different activities has also been suggested to allow evolution towards new catalytic activities [32,33•].

Warshel and colleagues have used EVB simulations to calculate free energy profiles for the reaction catalysed by alcohol dehydrogenase [10]. They calculated the contributions of $\Delta H^{\ddagger}$ and $\Delta S^{\ddagger}$ to the free energy barrier and showed that they were both temperature dependent. This temperature dependence was accentuated for the reaction with a deuterated substrate. These observations are sufficient to explain the increasingly curved Arrhenius plots for ADH with protiated and deuterated substrates, respectively. They proposed atomistic hypotheses for the experimental observations based on their calculations. The change in the temperature-dependence of $\Delta H^{\ddagger}$ between protiated and deuterated substrates is approximately 2.7 kJ·mol^{-1}·K^{-1}, far exceeding what is expected for an H to D substitution in the substrate. Formally, the temperature dependence of $\Delta H^{\ddagger}$ defines the activation heat capacity $\Delta C_P^{\ddagger}$ - the change in heat capacity between the ground state and the transition state along the reaction coordinate [29].

Pudney and colleagues observed a similar phenomenon for thermophilic glucose dehydrogenase (GDH): a single H to D substitution in the substrate changes $\Delta C_P^{\ddagger}$ for the reaction by a large amount: 2.3 kJ·mol^{-1}·K^{-1} [34]. Additional deuteration of the glucose substrate further reduces the magnitude of $\Delta C_P^{\ddagger}$ for the reaction (i.e. reduces the temperature dependence of $\Delta H^{\ddagger}$). $\Delta C_P^{\ddagger}$ was inferred by including this parameter in the Eyring equation and fitting temperature-rate data using this modified Eyring equation. Such large changes in heat capacity along the reaction coordinate arise because macromolecules such as enzymes can undergo significant changes in heat capacity due to conformational changes. These effects are explained by macromolecular rate theory (MMRT) [29].

Macromolecular Rate Theory
The activation heat capacity (at constant pressure) is defined as

$$\Delta C_P^{\ddagger} = \left(\frac{d\Delta H^{\ddagger}}{dT}\right)_P = T\left(\frac{d\Delta S^{\ddagger}}{dT}\right)_P \tag{2}$$

And this is related to the fluctuations in enthalpy and entropy via

$$\Delta\langle dH^2\rangle^\ddagger = k_B T^2 \Delta C_P^\ddagger, \quad \Delta\langle dS^2\rangle^\ddagger = k_B \Delta C_P^\ddagger \tag{3}$$

If an enzyme has two (or more) conformations in the ground state (as postulated by multiple authors, see above), which converge to one conformation at the transition state (Figure 1B), this will see a reduction in accessible conformations along the reaction coordinate and a negative value of the activation heat capacity $\Delta C_P^\ddagger$. Similarly, if $\Delta H^\ddagger$ is temperature dependent (as found e.g. by Warshel and colleagues [10]), this also implies that the activation heat capacity is non-zero. Where $\Delta C_P^\ddagger$ is different from zero the corresponding Arrhenius plot will be non-linear (Figure 1C).

Substituting equation 2 into the Eyring equation gives equation 4:

$$k_{cat} = \gamma(T) \frac{k_B T}{h} e^{\left(\frac{-\Delta G^\ddagger(T)}{k_B T}\right)} = \gamma(T) \frac{k_B T}{h} e^{\left(\frac{\Delta S_{T_0}^\ddagger + \Delta C_P^\ddagger(\ln T - \ln T_0)}{k_B}\right)} e^{\left(\frac{-\Delta H_{T_0}^\ddagger - \Delta C_P^\ddagger(T - T_0)}{k_B T}\right)} \tag{4}$$

and the corresponding curves for different values of $\Delta C_P^\ddagger$ can be seen in Figure 1C. There is good experimental evidence for MMRT from the temperature dependence of k_{cat} for a series of enzymes [35,36]. Additional evidence comes from direct measurement of ΔC_P for binding of transition state analogues to the enzyme methyl thioadenosine phophorylase (MTAP) using isothermal titration calorimetry (ITC) [37]. Molecular dynamics simulations yield values of $\Delta C_P^\ddagger$ that are commensurate with experiment for two very different enzymes [38••]. Values for $\Delta C_P^\ddagger$ were calculated from long-time scale MD simulations of the ground state (enzyme-substrate complex) and the transition state (enzyme-transition state analogue complex). An activation heat capacity indicates reduced energetic fluctuations at the transition state, indicating that transition state stabilization leads to a negative value of $\Delta C_P^\ddagger$ [39•] (Figure 2). Recent work from Hilvert and colleagues points towards the emergence of increasingly negative $\Delta C_P^\ddagger$ values for laboratory-evolved enzymes as they improve their catalytic proficiency [39•]. The heat capacity for any species is a function of the vibrational density of states for the species and thus, $\Delta C_P^\ddagger$ also reports on the changes in the distribution of vibrational states for an enzyme along the reaction coordinate.

Future Prospects

The critical role that temperature plays in enzyme function in the context of evolution (as well as in biotechnology) means that this field is very active. Enzyme crystal structures are often determined at artificially low temperatures, and this, along with averaging (as well as the crystal conditions) may disguise vibrational modes relevant for biology. X-ray crystallography [40] and cryo-EM [41] structures have now been determined at multiple temperatures (including room temperature) in order to tease out the possible changes in enzyme structure and dynamics with temperature. Recently, temperature jump experiments using small angle X-ray scattering (SAXS) as a detector have also been used to characterise enzyme dynamics [42•]. Temperature dependent conformational changes relevant to medicine are also being elucidated [43]. There is a growing recognition that investigations benefit significantly from bringing computational and experimental methods together to investigate the temperature dependence of enzyme-catalysed reaction rates [38,44]. Molecular simulations allow atomic-level analysis of protein dynamics and modelling of reactions (and e.g. transition states, see Figure 2), and calculations of thermodynamic properties such as activation enthalpies, entropies, and heat capacities [38]. They will be complemented by promising emerging approaches including incorporating machine learning to predict temperature optima for enzymes [45•].

2045 words

References

1.   Edwards DR, Lohman DC, Wolfenden R: **Catalytic proficiency: The extreme case of S-O cleaving sulfatases.** *J Am Chem Soc* 2012, **134**:525–531.

2.   Henri V: **Théorie générale de l'action de quelques diastases**. *C.R. Acad Sci Paris* 1902, **135**:916–919.

3.   Huggins DJ, Biggin PC, Dämgen MA, Essex JW, Harris SA, Henchman RH, Khalid S, Kuzmanic A, Laughton CA, Michel J, et al.: **Biomolecular simulations: From dynamics and mechanisms to computational assays of biological activity**. *WIREs Comput Mol Sci* 2018, **9**:e1393–23.

4.   Amaro RE, Mulholland AJ: **Multiscale methods in drug design bridge chemical and biological complexity in the search for cures**. *Nat Rev Chem* 2018, **2**:0148.

5.••   Sočan J, Isaksen GV, Brandsdal BO, Åqvist J: **Towards rational computational engineering of psychrophilic enzymes.** *Sci Rep* 2019, **9**:19147.

       An approach to enzyme engineering using advanced computational techniques and incorporating previous advances in understanding of the temperature dependence of psychrophilic enzymes. Specifically, surface loops are engineered to alter the temperature dependence of elastase enzymes via an enthalpy-entropy tradeoff.

6.   Akanuma S, Bessho M, Kimura H, Furukawa R, Yokobori S-I, Yamagishi A: **Establishment of mesophilic-like catalytic properties in a thermophilic enzyme without affecting its thermal stability.** *Sci Rep* 2019, **9**:9346.

7. •• Iorgu AI, Baxter NJ, Cliff MJ, Levy C, Waltho JP, Hay S, Scrutton NS: **Nonequivalence of second sphere "noncatalytic" residues in pentaerythritol tetranitrate reductase in relation to local dynamics linked to H-transfer in reactions with NADH and NADPH coenzymes**. *ACS Catalysis* 2018, **8**:11589–11599.

       A multipronged experimental investigation of the temperature dependence of pentaerythritol tetranitrate reductase (PETNR) using mutagenesis, multiple substrates, stopped flow kinetics, kinetic isotope effects, and NMR. The combination of enzyme mutagenesis and NADH/NADPH coenzymes provides a rich dataset upon which to formulate hypotheses regarding the molecular details of thermal adaptation for this enzyme.

8.   Kamerlin SCL, Warshel A: **At the dawn of the 21st century: Is dynamics the missing link for understanding enzyme catalysis?** *Proteins: Struct Func Bioinfo* 2010, **78**:1339–1375.

9.   Glowacki DR, Harvey JN, Mulholland AJ: **Taking Ockham's razor to enzyme dynamics and catalysis.** *Nat Chem* 2012, **4**:169–176.

10. •• Roy S, Schopf P, Warshel A: **Origin of the non-Arrhenius behavior of the rates of enzymatic reactions.** *J Phys Chem B* 2017, **121**:6520–6526.

Using empirical valence bond (EVB) simulations, free energy barriers for the reaction catalysed by alcohol dehydrogenase are calculated. Classical contributions to the free energy barrier from entropy ($\Delta S^{\ddagger}$) are shown to be temperature dependent. They further suggest that changes to the entropic contributions from nuclear quantum effects primarily contribute at low temperatures, related to the donor-acceptor distance.

11.   Åqvist J, Isaksen GV, Brandsdal BO: **Computation of enzyme cold adaptation**. *Nat Rev Chem* 2017, **1**:0051–14.

12.   Wolfenden R: **Massive thermal acceleration of the emergence of primordial chemistry, the incidence of spontaneous mutation, and the evolution of enzymes.** *J Biol Chem* 2014, **289**:30198–30204.

13.   Truhlar DG: **Transition state theory for enzyme kinetics.** *Arch Biochem Biophys* 2015, **582**:10–17.

14.   Garcia-Viloca M, Gao J, Karplus M, Truhlar DG: **How enzymes work: analysis by modern rate theory and computer simulations**. *Science* 2004, **303**:186–195.

15.   Somero GN: **Adaptation of enzymes to temperature: searching for basic "strategies".** *Comp Biochem Physiol B, Biochem Mol Biol* 2004, **139**:321–333.

16.   Ruiz-Pernía JJ, Tuñón I, Moliner V, Allemann RK: **Why Are Some Enzymes Dimers? Flexibility and Catalysis in Thermotoga maritima Dihydrofolate Reductase**. *ACS Catalysis* 2019, **9**:5902–5911.

17.   Wintrode PL, Arnold PH: **Temperature adaptation of enzymes: Lessons from laboratory evolution**. *Adv Protein Chem* 2001, **55**:161–225.

18.   Miyazaki K, Wintrode PL, Grayling RA, Rubingh DN, Arnold FH: **Directed evolution study of temperature adaptation in a psychrophilic enzyme.** *J Mol Biol* 2000, **297**:1015–1026.

19.   Berg K, Leiros I, Williamson A: **Temperature adaptation of DNA ligases from psychrophilic organisms**. *Extremophiles* 2019, **23**:305–317.

20.   Saavedra HG, Wrabl JO, Anderson JA, Li J, Hilser VJ: **Dynamic allostery can drive cold adaptation in enzymes**. *Nature* 2018, **558**:324–328.

21.   Arcus VL, Mulholland AJ: **Temperature, dynamics, and enzyme-catalyzed reaction rates.** *Annu Rev Biophys* 2020, **49**:163-80.

22.   Struvay C, Feller G: **Optimization to low temperature activity in psychrophilic enzymes**. *Int J Mol Sci* 2012, **13**:11643–11665.

23.   Åqvist J, Kazemi M, Isaksen GV: **Entropy and enzyme catalysis**. *Acc Chem Res* 2017, **50**:199-207.

24. • Sočan J, Kazemi M, Isaksen GV, Brandsdal BO, Åqvist J: **Catalytic adaptation of psychrophilic elastase.** *Biochemistry* 2018, **57**:2984–2993.

The companion paper to [5] above describing the initial extensive EVB calculations on psychrophilic salmon and mesophilic porcine elastase enzymes. The calculations show the redistribution of enthalpy and entropy contributions to the free energy barrier ($\Delta G^{\ddagger}$) for the psychrophilic enzyme and this is linked to the mobility of surfaces exposed loops.

25. Feller G: **Psychrophilic enzymes: From folding to function and biotechnology.** *Scientifica* 2013, **2013**:1–28.

26. Kavanau JL: **Enzyme kinetics and the rate of biological processes.** *J Gen Physiol* 1950, **34**:193–209.

27. Massey V, Curti B, Ganther H: **A temperature-dependent conformational change in D-amino acid oxidase and its effect on catalysis.** *J Biol Chem* 1966, **241**:2347–2357.

28. Truhlar DG, Kohen A: **Convex Arrhenius plots and their interpretation.** *Proc Natl Acad Sci USA* 2001, **98**:848–851.

29. Arcus VL, Prentice EJ, Hobbs JK, Mulholland AJ, van der Kamp MW, Pudney CR, Parker EJ, Schipper LA: **On the temperature dependence of enzyme-catalyzed rates.** *Biochemistry* 2016, **55**:1681–1688.

30. Daniel RM, Danson MJ: **A new understanding of how temperature affects the catalytic activity of enzymes.** *Trends Biochem Sci* 2010, **35**:584–591.

31. Changeux J-P: **Allostery and the Monod-Wyman-Changeux model after 50 years.** *Annu Rev Biophys* 2012, **41**:103–133.

32. Campbell E, Kaltenbach M, Correy GJ, Carr PD, Porebski BT, Livingstone EK, Afriat-Jurnou L, Buckle AM, Weik M, Hollfelder F, et al.: **The role of protein dynamics in the evolution of new enzyme function.** *Nat Chem Biol* 2016, **12**:944–950.

33. • Petrović D, Risso VA, Kamerlin SCL, Sanchez-Ruiz JM: **Conformational dynamics and enzyme evolution.** *J Royal Soc Interface* 2018, **15**:20180330–18.

An excellent review of data for several enzymes specifically from the point of view of conformational dynamics and enzyme evolution. The hypothesis that conformational dynamics makes rare, promiscuous activities accessible to evolution is presented.

34. Jones HBL, Crean RM, Matthews C, Troya AB, Danson MJ, Bull SD, Arcus VL, van der Kamp MW, Pudney CR: **Uncovering the relationship between the change in heat capacity for enzyme catalysis and vibrational frequency through isotope effect studies.** *ACS Catalysis* 2018, **8**:5340–5349.

35.   Arcus VL, Pudney CR: **Change in heat capacity accurately predicts vibrational coupling in enzyme catalyzed reactions.** *FEBS Lett* 2015, **589**:2200–2206.

36.   Longbotham JE, Hardman SJO, Görlich S, Scrutton NS, Hay S: **Untangling heavy protein and cofactor isotope effects on enzyme-catalyzed hydride transfer.** *J Am Chem Soc* 2016, **138**:13693–13699.

37.   Firestone RS, Cameron SA, Karp JM, Arcus VL, Schramm VL: **Heat capacity changes for transition-state analogue binding and catalysis with Human 5'-Methylthioadenosine Phosphorylase.** *ACS Chem Biol* 2017, **12**:464–473.

38. ••   van der Kamp MW, Prentice EJ, Kraakman KL, Connolly M, Mulholland AJ, Arcus VL: **Dynamical origins of heat capacity changes in enzyme-catalysed reactions.** *Nat Commun* 2018, **9**:1177.

        A computational molecular dynamics investigation of two diverse enzymes (large monomeric, small dimeric) using the fluctuations in enthalpy at the reactant state and the transition state to calculate the activation heat capacity ($\Delta C_P^{\ddagger}$, see equation 3). The calculated values were commensurate with experimental values determined from the temperature dependence of the catalytic rate constant. Notably, contributions to ($\Delta C_P^{\ddagger}$) arise from all parts of the enzyme including the dimeric partner and auxiliary domains.

39. •   Bunzel HA, Kries H, Marchetti L, Zeymer C, Mittl PRE, Mulholland AJ, Hilvert D: **Emergence of a negative activation heat capacity during evolution of a designed enzyme.** *J Am Chem Soc* 2019, 141:11745-48.

        Experimental directed evolution of a designed enzyme suggests that as the rate enhancement increases, activation heat capacity becomes more negative. This is consistent with the hypothesis that stabilization of the transition state leads to a narrowing of the enthalpic fluctuations at this state when compared to the ground state. It is also consistent with an enthalpy-entropy tradeoff in enzyme evolution.

40.   Horrell S, Kekilli D, Sen K, Owen RL, Dworkowski FSN, Antonyuk SV, Keal TW, Yong CW, Eady RR, Hasnain SS, et al.: **Enzyme catalysis captured using multiple structures from one crystal at varying temperatures**. *IUCrJ* 2018 M5, 283-292.

41.   Chen C-Y, Chang Y-C, Lin B-L, Huang C-H, Tsai M-D: **Temperature-resolved cryo-EM uncovers structural bases of temperature-dependent enzyme functions.** *J Am Chem Soc* 2019, **141**:19983–19987.

42. •   Thompson MC, Barad BA, Wolff AM, Sun Cho H, Schotte F, Schwarz DMC, Anfinrud P, Fraser JS: **Temperature-jump solution X-ray scattering reveals distinct motions in a dynamic enzyme.** *Nat Chem* 2019, **11**:1058–1066.

        Temperature-jump experiments for cyclophilin A using small- and wide-angle X-ray scattering as the detector. Rich dynamics on the microsecond timescale are revealed by this approach.

43.   Deredge D, Wintrode PL, Tulapurkar ME, Nagarsekar A, Zhang Y, Weber DJ, Shapiro P, Hasday JD: **A temperature-dependent conformational shift in p38α MAPK substrate–binding region associated with changes in substrate phosphorylation profile**. *J Biol Chem* 2019, **294**:12624–12637.

44.   Zaragoza JPT, Nguy A, Minnetian N, Deng Z, Iavarone AT, Offenbacher AR, Klinman JP: **Detecting and characterizing the kinetic activation of thermal networks in proteins: Thermal transfer from a distal, solvent-exposed loop to the active site in Soybean Lipoxygenase**. *J Phys Chem B* 2019, **123**:8662–8674.

45. •   Li G, Rabe KS, Nielsen J, Engqvist MKM: **Machine learning applied to predicting microorganism growth temperatures and enzyme catalytic optima**. *ACS Synth Biol* 2019, **8**:1411–1420.

        Machine learning based on 2-mer amino acid composition for the whole proteome can accurately predict the optimal growth temperature for oranisms and further, the optimal temperature for enzyme-catatlysed reaction rates.
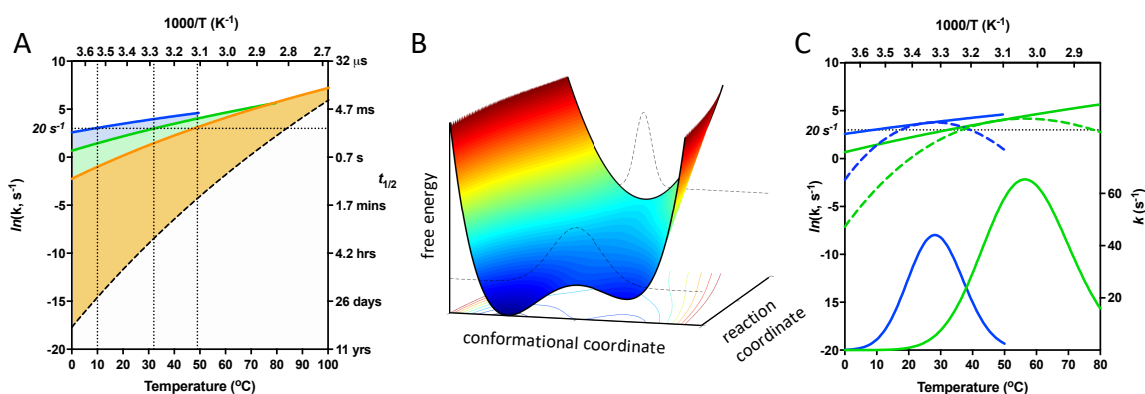
Figure 1. A. The temperature dependence of uncatalyzed and enzyme-catalyzed reaction rates. A hypothetical chemical reaction rate (y axis, log scale) varies with temperature (x axis) according to the Eyring equation (Equation 1), assuming $\gamma(T) = 1$. The uncatalyzed reaction is shown as a dashed line ($\Delta H^{\ddagger} = 147$ kJ.mol^{-1}, $\Delta S^{\ddagger} = 195$ J.mol^{-1}.K^{-1}). Enzyme-catalyzed reaction rates (for the same reaction) are shown for hypothetical psychrophilic (*blue*, $\Delta H^{\ddagger} = 27.4$ kJ.mol^{-1}, $\Delta S^{\ddagger} = -122.4$ J.mol^{-1}.K^{-1}), mesophilic (*green*, $\Delta H^{\ddagger} = 47.4$ kJ.mol^{-1}, $\Delta S^{\ddagger} = -65.1$ J.mol^{-1}.K^{-1}), and thermophilic enzyme homologs (*red*, $\Delta H^{\ddagger} = 77$ kJ.mol^{-1}, $\Delta S^{\ddagger} = 20.6$ J.mol^{-1}.K^{-1}). The rate enhancement is illustrated by shading. The gentle curvature is a result of using a linear temperature scale (as opposed to the inverse temperature scale typical of an Arrhenius plot – the inverse temperature is shown on the upper x axis). Enzymes have evolved to show similar rates at their environmental temperatures, and this is illustrated by a horizontal line at 20 s^{-1} and the x axis intercepts for each enzyme (indicating hypothetical environmental temperatures for thermophile, mesophile, and psychrophile). The decreasing slopes for the uncatalyzed rate and thermophilic, mesophilic, and psychrophilic enzyme-catalyzed rates illustrates the enthalpy–entropy trade-off as enzymes evolve to catalyze reactions at lower temperatures. Half-life values (t$_{1/2}$) are shown on the right-hand y axis. **B.** A change in heat capacity for an enzyme-catalyzed reaction. A hypothetical free energy surface is shown with two distinct conformations in the reactant state illustrated by two shallow energy wells. The fluctuations in enthalpy for this state and the transition state are depicted by Gaussians (*dashed lines above surface*). The transition state is at higher energy, and the fluctuations at this state are narrower. The consequences of this are shown in **C.** The temperature dependence of the hypothetical psychrophilic and mesophilic enzyme-catalyzed rates are reproduced from **A.** However, if there is a change in heat capacity along the reaction coordinate, as illustrated in **B.**, then the observed temperature dependence will be according to the dashed lines of the same color ($\Delta C_p^{\ddagger} = -10$ and -5 kJ.mol^{-1}.K^{-1} for psychrophilic and mesophilic enzymes, respectively). The absolute rates that correspond to these dashed lines are shown in solid lines at the bottom and on the right-hand y axis. Note that the optimum temperature for the psychrophile is now 28 °C, and that for the mesophile is 60 °C, in the absence of denaturation. Figure adapted from [21] with permission.
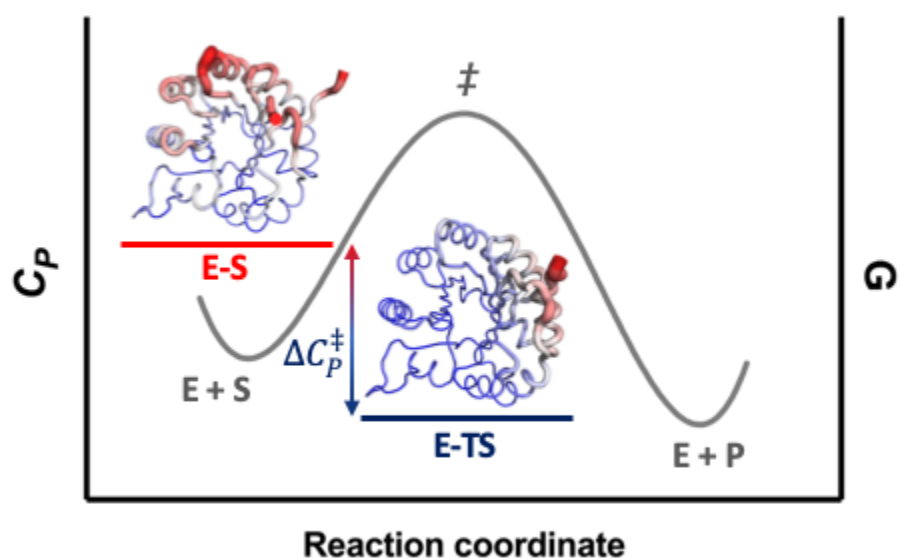
Figure 2. A schematic illustrating the enzyme-catalyzed reaction coordinate proceeding from enzyme + substrate (E+S) to enzyme + products (E+P) via the transition state ($\ddagger$). The Gibbs free energy (G) is on the right-hand y-axis and corresponds to the grey line. The heat capacity (C_P) is on the left-hand y-axis. The root-mean-square fluctuations (RMSF) for the enzyme-substrate and enzyme-transition state complexes are depicted by both colour (blue to red) and tube width. This shows that the RMSF values are significantly reduced for a large fraction of the enzyme upon proceeding from the E-S complex to the E-TS complex and this results in large, negative values for the activation heat capacity.